Physiol. Res. 73 (Suppl. 1): S471-S476, 2024 *https://doi.org/10.33549/physiolres.935292*

REVIEW

Mathematical Models of Diffusion in Physiology

Jiří JANÁČEK[1]

[1]Laboratory of Biomathematics, Institute of Physiology of the Czech Academy of Sciences, Praha 4, Czech Republic

Received November 30, 2023
Accepted January 2, 2024

Summary

Diffusion is a mass transport phenomenon caused by chaotic thermal movements of molecules. Studying the transport in specific domain is simplified by using evolutionary differential equations for local concentration of the molecules instead of complete information on molecular paths [1]. Compounds in a fluid mixture tend to smooth out its spatial concentration inhomogeneities by diffusion. Rate of the transport is proportional to the concentration gradient and coefficient of diffusion of the compound in ordinary diffusion. The evolving concentration profile $c(x,t)$ is then solution of evolutionary partial differential equation

$$\frac{\partial c}{\partial t} = D\Delta c$$

where D is diffusion coefficient and Δ is Laplacian operator. Domain of the equation may be a region in space, plane or line, a manifold, such as surface embedded in space, or a graph. The Laplacian operates on smooth functions defined on given domain. We can use models of diffusion for such diverse tasks as: a) design of method for precise measurement of receptors mobility in plasmatic membrane by confocal microscopy [2], b) evaluation of complex geometry of trabeculae in developing heart [3] to show that the conduction pathway within the embryonic ventricle is determined by geometry of the trabeculae.

Key words

Diffusion • Mathematical modeling • FRAP • Plasma membrane • Trabeculation

Corresponding author

J. Janáček, Laboratory of Biomathematics, Institute of Physiology CAS, Vídeňská 1083, 14200 Praha 4, Czech Republic. E-mail: Jiri.Janacek@fgu.cas.cz

Introduction

Energy of thermal molecular movements is distributed into various modes according to configuration and environment of the molecules. Besides rotational and vibrational modes there are thermal molecular translations, chaotic motions causing the phenomenon of diffusion. The speed of the ordinary diffusion is fully characterized by diffusion coefficient (D) [1]. Ordinary diffusion takes place in homogeneous environment and the diffusion in structured or compartmentalized environment is usually anomalous. Anomalies in diffusion can be utilized for studying the underlying structure, for example, mean square displacement (MSD) of a particle, which is linear function of time in ordinary diffusion ($MSD(t) = D\,t$), can serve this purpose.

Specific methods of optical microscopy study molecular translations on scales ranging from single molecule up to the size of field of view.

Single fluorescently labelled molecule can be tracked in real time by superresolution microscope Minflux [4]. This method provides real path of the molecule, hence all parameters of the movements can be calculated, but very special equipment is needed and it tracks only one target at a time.

Fluorescence fluctuation techniques follow fluctuation of local concentration of the molecules. Fluorescence correlation spectroscopy (FCS) calculates diffusion coefficient D from time correlations of fluorescence in static focal volume [5]. Methods based on spatiotemporal correlations of fluorescence (ImCS) [6] provide information on anomalies in diffusion in MSD function. Those techniques require very low

concentration of fluorophores (i.e. dim fluorescence), units to tens molecules per focal volume, to obtain fluctuating fluorescence signals.

Methods operating in coarsest spatial scale calculate the diffusion coefficient D (or apparent D if the diffusion is in fact anomalous) from time evolution of the molecules concentration profile. Widely used is fluorescence recovery after photobleaching (FRAP) [5,7]. We analyzed dynamics of receptors on plasmatic membranes by FRAP on periphery of cell. We developed customized model of bleaching and diffusion in vertical plane in order to evaluate properly the FRAP experiment using microscopic objective with high numerical aperture [2].

Mathematical model of the evolving concentration profile is partial differential equation (PDE) of diffusion on a given domain. The diffusion coefficient D is calculated by fitting model FRAP curve to the measured one.

Properties of the Laplacian operator reflect form (i.e. dimension, shape and size) of the equation domain. Regular domains in Euclidean spaces [8,9] and fractal domains [10] were characterized by asymptotic properties of the operator eigenvalues.

We studied geometry of trabeculation in developing mouse embryonic heart using solutions of diffusion equation on graph obtained by skeletonization of the trabeculae. The directionality of the trabeculae was calculated from directionality of the equation solutions. [3]. The connectivity of the trabecular graph was characterized by fracton dimension estimated from asymptotics of the Laplacian operator eigenvalues.

Equations of diffusion

The Laplacian operator in one dimension (along line) is

$$\Delta c = \frac{\partial^2 c}{\partial x^2}$$

hence, the simplest (one-dimensional) equation of diffusion along line is

$$\frac{\partial c}{\partial t} = D\frac{\partial^2 c}{\partial x^2}$$

The equation has special solutions, so called Green functions, centered in point y

$$\frac{1}{2\sqrt{\pi Dt}} e^{-\frac{(x-y)^2}{4Dt}}$$

and we obtain diffusion profile $c(x,t)$ evolving from arbitrary initial profile $c(x,0)$ by integration

$$\frac{1}{2\sqrt{\pi Dt}} \int_{-\infty}^{\infty} e^{-\frac{(x-y)^2}{4Dt}} c(x,0)dy$$

For example, the profile evolving from $c(x,0)$, concentration equal to zero in interval from $-l/2$ to $l/2$ and equal to one elsewhere (Fig. 1a), can be expressed explicitly by formula

$$c(x,t) = 1 - \frac{1}{2}\left(Erf\frac{\left(\frac{l}{2} - x\right)}{2\sqrt{Dt}} + Erf\frac{\left(\frac{l}{2} + x\right)}{2\sqrt{Dt}} \right)$$

[11], where $Erfy = \int_0^y e^{-z^2}\, dz$ is error function.

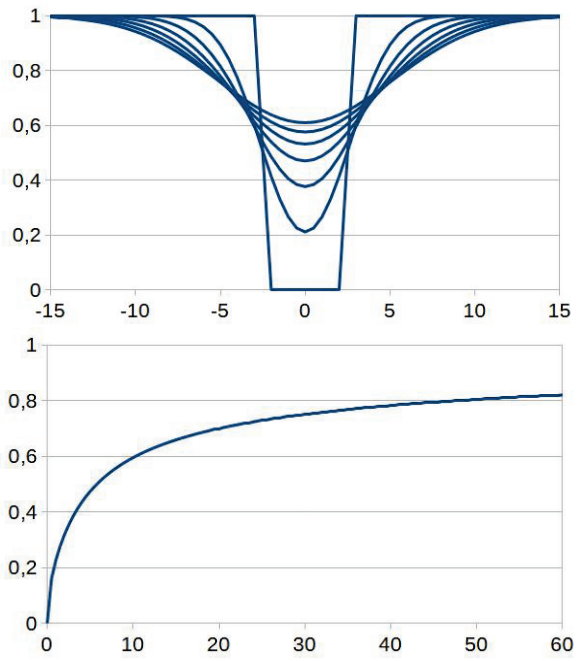

Fig. 1. (**a**) Concentration profile evolving in time, D=1. l=5. Time step 2 s. (**b**) Integral of the profile from -2,5 to 2,5 as function of time.

Diffusion of fluorescent receptors on vertical plasmatic membrane

Mobility of fluorescent molecules is studied by microscopic technique called fluorescence recovery after photobleaching (FRAP). Region of interest (ROI) in the target object is irreversibly bleached and then we record the light recovered by flow of fluorescent molecules into ROI.

FRAP along a tubule, e.g. neurite can be evaluated by fitting one-dimensional model curve to the recorded data

$$F(t) = F_0 + (F_\infty - F_0)F(Dt)$$

where F_0 is the postbleach value of F and F_∞ is the limit at infinity and F is calculated from the ordinary diffusion model (with D=1) as the amount of matter transported into the interval from $-l/2$ to $l/2$ up to time t by the integral of the concentration profile over the interval

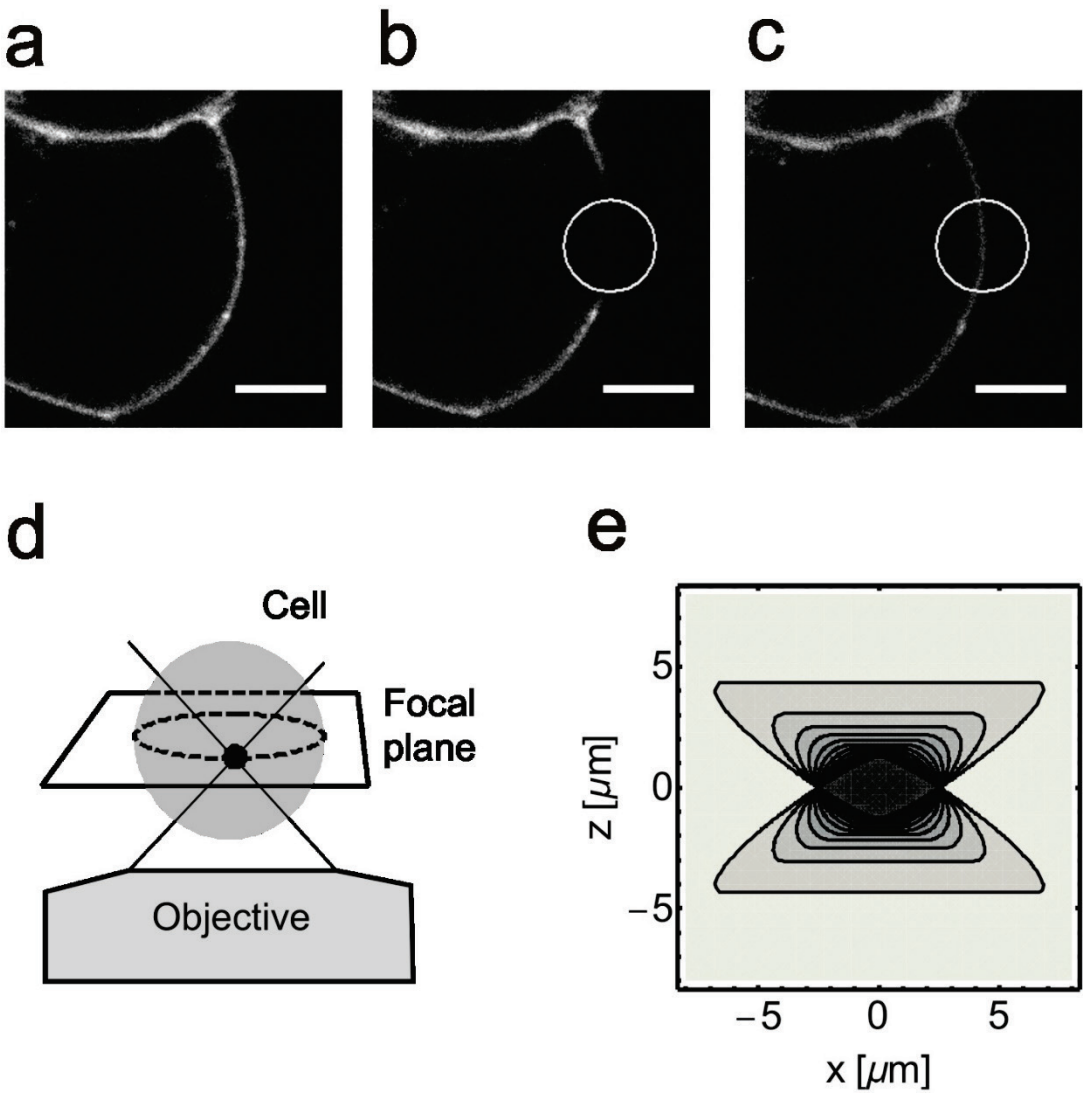

Fig. 2. FRAP measurement of plasma membrane protein mobility using „equatorial set-up". (**a-c**) Confocal images of the HEK293 cell expressing δ-OR-eYFP in the course of FRAP experiment: the optical section of the cell before the bleach (**a**), shortly after the bleach (**b**) and after the recovery of fluorescence signal in the bleached region of interest (ROI) (**c**). The white circle in b and c represents ROI used for recording the fluorescence recovery curve. Scale bars represent 5 μm. (**d**) Scheme of confocal imaging of plasma membrane region within the equatorial plane of the cell. (**e**) Axial profile of photobleaching irradiance calculated for horizontal circular ROI with diameter of 5 μm and water immersion objective with numerical aperture (NA) 1,2.

(Fig. 1b), which can be expressed in closed form as

$$F(t) = 1 - \frac{2\sqrt{t}}{l\sqrt{\pi}}\left(e^{-\frac{l^2}{4t}} - 1\right) - Erf\,\frac{l}{2\sqrt{t}}$$

See 7.2 in [12] for integral of *Erf*.

Mobility of molecules constrained to plasmatic membrane may be assessed by FRAP. The signal from plasmatic membrane with ROI on the periphery of the cell (Fig. 2a,b,c) obtained by confocal microscope equipped with objective with high numerical aperture cannot be analyzed neither by the above 1 dimensional model nor by other models found in FRAP literature [13], because the cone of light from high NA objective has obtuse apical angle and the bleached region on the horizontal plane approximating the plasma membrane (Fig. 2d) has hour-glass shape [14]. Analysis of FRAP of fluorescently labelled opioid receptors thus required development of new specific model [2]. We started with analytical expression for irradiance $I(x, z)$ applied in the bleaching in circular ROI (Fig. 2e) where horizontal coordinate x and axial coordinate z have origin in the center of ROI (see Appendix and [2] for details).

Concentration of fluorophore $c(x, z, t)$ in vertical x, z-plane obeys the diffusion equation:

$$\frac{\partial c}{\partial t} = D\left(\frac{\partial^2 c}{\partial x^2} + \frac{\partial^2 c}{\partial z^2}\right)$$

where D is the diffusion coefficient.

The initial, normalized concentration of fluorophore is calculated from 3D irradiation intensity

$I(x,z)$ (defined in Appendix) by formula:

$$c(x,z,0) = e^{-\alpha T\, I(x,z)}$$

where α is rate constant and T is duration of the bleaching pulse. Let $D = 1$.

$$c(x,z,t) = \frac{1}{4\pi t}\int_{-\infty}^{\infty}\int_{-\infty}^{\infty} e^{-\frac{(x-\xi)^2+(z-\zeta)^2}{4t}} c(x,z,0)d\xi\, d\zeta$$

Let $K = \alpha T\, I$ [7], the model FRAP recovery curve F_K is then obtained by integration of the fluorophore concentration over the linear segment,

$$F_K(t) = \frac{1}{2R}\int_{-R}^{R} c(x,0,t)dx$$

which is equal to:

$$F_K(t) = \frac{1}{8R\sqrt{\pi t}}\int_{-\infty}^{\infty} e^{-\frac{z^2}{t}} J_K(z,t)dz$$

where

$$J_K(z,t) = \int_{-\infty}^{\infty}\left(Erf\frac{R-x}{2\sqrt{t}} + Erf\frac{R+x}{2\sqrt{t}}\right)e^{-\alpha T I(x,z)}dx$$

The double integral in equation for F_K (t) is evaluated for using a numerical procedure in program *Mathematica (Wolfram)*. The example of F_K (t) curves is depicted in Figure 3a.

Experimental FRAP curve, such as that at Figure 3b, is fitted by function

$$F(t) = F_\infty F_K(Dt)$$

where F_∞ is the limit at infinity.

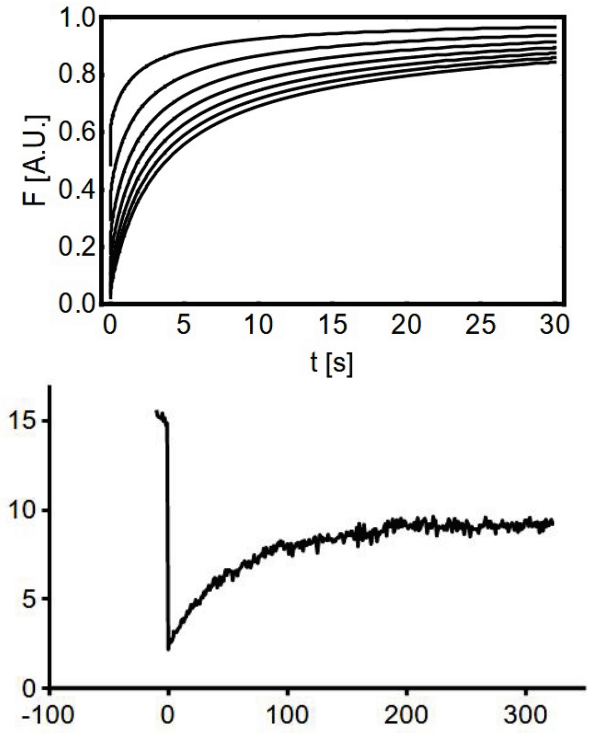

Fig. 3. (**a**) Simulated fluorescence recovery (FRAP) curves for various values of bleaching intensity K=0,5 to 3,5, numerical aperture NA=1,2, refractive index n=1,33 and diffusion coefficient D=1. (**b**) an example of real FRAP signal from plasmatic membrane on the periphery of cell.

Directionality of trabeculae in embryonic heart

Trabeculae in embryonic heart of Nkx-2.5:GFP mice were visualized in 3D using confocal microscope with 10× dry objective [3].

The binary image obtained by segmentation of the original image was skeletonized obtaining the graph (Fig. 4a) representing the trabeculae.

Local anisotropy of the trabecular structure is characterized by directionality of heat conduction, or equivalently by directionality of Brownian motion. For this purpose we use the graph $G = (V, E)$ with edges weighted by s- "conductance" (equal to reciprocal distance)

$$s(v_i, v_j) = \|v_i - v_j\|^{-1}$$

as the model of the trabecular structure.

The graph Laplacian Δ is I × I matrix with elements

$$\Delta_{ii} = -\sum_{(v_i,v_j)\in E} r(v_i, v_j)$$

$$\Delta_{ij} = r(v_i, v_j) \text{ if } i \neq j \text{ for } (v_i, v_j) \in E$$

$$\text{and } \Delta_{ij} = 0 \text{ for } (v_i, v_j) \notin E$$

The Laplacian is employed in formulation of the diffusion equation on the graph:

$$\frac{\partial c}{\partial t}(v,t) = \Delta c(v,t),\ \ v \in V, t \geq 0.$$

λ_n- eigenvalues and φ_n- orthonormal eigenvectors of the graph Laplacian Δ are related by equations

$$\Delta\varphi_n = \lambda_n\varphi_n, n = 1 \ldots I$$

so that $e^{\lambda_n t}\varphi_n(v)$ are generators of solutions of the diffusion equation.

The Green functions of the diffusion equation are defined using the eigenvectors and eigendomains as:

$$K(x,y,t) = \sum_{n=1}^{I} \varphi_n(x)\varphi_n(y)e^{\lambda_n t}$$

Second moments of the Green function in each point $y \in V$ can be calculated as:

$$T_{lk}(y,t) = \sum_{x\in V}\sum_{n=1}^{I} \varphi_n(y)\varphi_n(x)e^{\lambda_n t}(x_l - y_l)(x_k - y_k)$$

$$l, k = 1,2,3$$

Eigenvalues were calculated by DSBEVX routine in LAPACK library [15].

Eigenvectors were calculated by inverse iterations:

$$(\Delta - \lambda I)\varphi = b_m$$

$$b_{m+1} = \pm\frac{\varphi}{\|\varphi\|}$$

using LU decomposition from Numerical Recipes [16]. The tensor of the heat kernel second moments $T(y,t)$ was calculated, the values were interpolated and

visualized (Fig. 4b) in Amira 6.5 (FEI) using the module Tensor View.

Eigenvalues λ_n were distributed as $n^{\frac{2}{d}}$, where d correspond to (fractal) dimension growing from value 2.1 at ED10 to 2.5 at ED14.

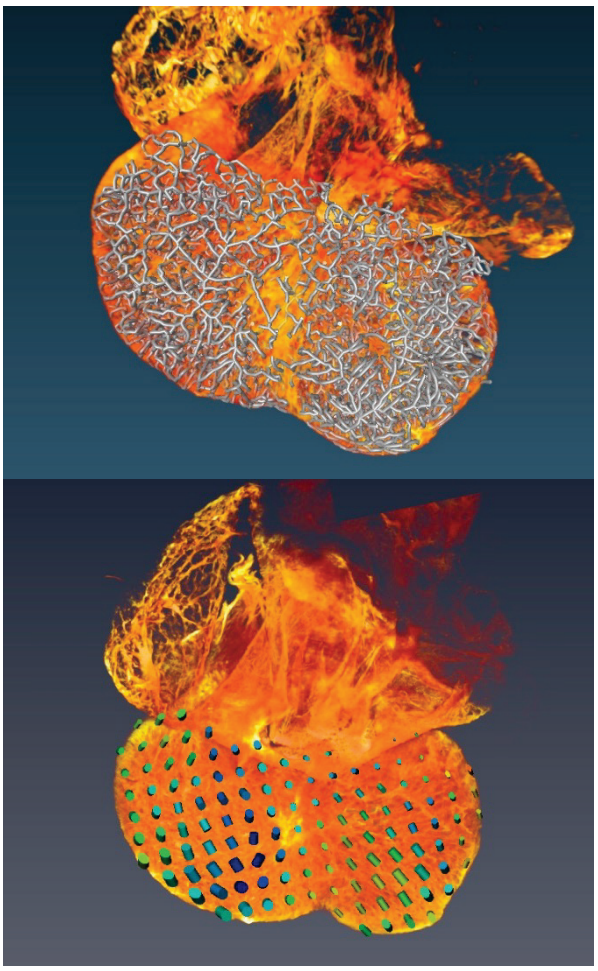

Fig. 4. (**a**) Graph of skeletonized trabeculae in mouse embryonic heart. (**b**) directionality tensor of diffusion on the graph.

Discussion and Conclusions

We demonstrated custom made FRAP model for evaluation of receptor mobility measured on periphery of cell by microscope with high numerical aperture. Using precise model is necessary, because 1D model, that is used for evaluation of this experiment with objective with low numerical aperture, would overestimate the value of diffusion coefficient by factor of two.

The history of the study of asymptotics of Laplacian operator eigenvalue in relation to its domain is long and interesting. First results were obtained in theoretical studies on radiation of the dark body [8] and they were completed by results on vibrational modes of solid bodies [9] and of fractals [10]. Trabeculae in embryonic heart have complicated structure of open foam that is difficult to characterize by conventional geometrical parameters. Dimension calculated from asymptotics of Laplacian eigenvalues somehow characterizes local connectivity of the structure, that is slightly lower than that of regular 3D grid. Fractal characterization of heart trabeculae were used also by others [17] and it can be applied in future to characterization of other complicated biological structures and network like objects.

Conflict of Interest

There is no conflict of interest.

References

1. Einstein A. Über die von der molekularkinetischen Theorie der Wärme geforderte Bewegung von in ruhenden Flüssigkeiten suspendierten Teilchen. Ann Phys 1905;17:549-560. https://doi.org/10.1002/andp.19053220806
2. Janáček J, Brejchová J, Svoboda P. Determination of delta-opioid receptor molecules mobility in living cells plasma membrane by novel method of FRAP analysis. Biochim Biophys Acta Biomembr 2019;1861:1346-1354. https://doi.org/10.1016/j.bbamem.2019.04.012
3. Olejníčková V, Šaňková B, Sedmera D, Janáček J: Trabecular architecture determines impulse propagation through the early embryonic mouse heart. Front Physiol 2019;9:1876. https://doi.org/10.3389/fphys.2018.01876
4. Balzarotti F, Eilers Y, Gwosch KC, Gynnå AH, Westphal V, Stefani FD, Elf J, Hell SW. Nanometer resolution imaging and tracking of fluorescent molecules with minimal photon fluxes. Science 2017;355:606-612. https://doi.org/10.1126/science.aak9913
5. Koppel DE, Axelrod D, Schlessinger J, Elson E, Webb WW, Dynamics of fluorescence marker concentration as a probe of mobility. Biophys J 1976;16:1315-1329. https://doi.org/10.1016/S0006-3495(76)85776-1

6. Planes N, Vanderheyden PPML, Gratton E, Caballero-George C. Image mean square displacement to study the lateral mobility of Angiotensin II type 1 and Endothelin 1 type A receptors on living cells. Microsc Res Tech 2020;83:381-392. https://doi.org/10.1002/jemt.23425
7. Axelrod D, Koppel DE, Schlessinger J, Elson E, Webb WW. Mobility measurements by analysis of fluorescence photobleaching recovery kinetics. Biophys J 1976;16:1055-1069. https://doi.org/10.1016/S0006-3495(76)85755-4
8. Weyl H. Das asymptotische Verteilungsgesetzt der Eigenverte linearer partieller Differentialgleichungen (mit einer Anwendung auf die Theorie der Hohlraumstrahlung). Math Ann 1912;71:441-479. https://doi.org/10.1007/BF01456804
9. Kac M. Can one hear the shape of a drum? Am Math Month 1966;73.4/2:1-23. https://doi.org/10.1080/00029890.1966.11970915
10. Alexander S, Orbach R. Density of states on fractals: fractons. J Phys Lett 1982;43:625-631. https://doi.org/10.1051/jphyslet:019820043017062500
11. Crank J. The Mathematics of Diffusion, Clarendon Press, 1956.
12. Abramowitz M, Stegun I. Handbook of Mathematical Functions with Formulas, Graphs, and Mathematical Tables. United States Department of Commerce, National Bureau of Standards, 1964.
13. Loren N, Hagman J, Jonasson JK, Deschout H, Bernin D, Cella-Zanacchi F, Diaspro A, McNally JG, Ameloot M, Smisdom N, Nyden M, Hermansson AM, Rudemo M, Braeckmans K, Fluorescence recovery after photo-bleaching in material and life sciences: putting theory into practice. Q Rev Biophys 2015;48:323-387. https://doi.org/10.1017/S0033583515000013
14. Mazza D, Cella F, Vicidomini G, Krol S, Diaspro A. Role of three-dimensional bleach distribution in confocal and two-photon fluorescence recovery after photobleaching experiments. Appl Opt 2007;46:7401-7411. https://doi.org/10.1364/AO.46.007401
15. Anderson E, Bai Z, Bischof C, Blackford S, Demmel J, Dongarra J, Du Croz J, Greenbaum A, Hammarling S, McKenney A, Sorensen D. LAPACK Users' Guide. Third ed. Philadelphia, Society for Industrial and Applied Mathematics; 1999. https://doi.org/10.1137/1.9780898719604
16. Press WH, Teukolsky SA, Vetterling WT, Flannery BP. Numerical recipes in C : the art of scientific computing, Second ed. Cambridge, New York, Cambridge University Press, 1992.
17. Meyer HV, Dawes TJW, Serrani M, Bai W, Tokarczuk P, Cai J, de Marvao A, Henry A, Lumbers RT, Gierten J, Thumberger T, Wittbrodt J, Ware JS, Rueckert D, Matthews PM, Prasad SK, Costantino ML, Cook SA, Birney E, O'Regan DP. Genetic and functional insights into the fractal structure of the heart. Nature 2020;584:589-594. https://doi.org/10.1038/s41586-020-2635-8

Appendix

Let n be refractive index of the immersion media, let β be half angle of the objective light cone satisfying the relation $NA = n \sin\beta$ for numerical aperture NA of the objective and let region of interest (ROI) be a circle with radius R, then $I(r, z)$, where horizontal coordinate $r>0$ and axial coordinate z have origin in the center of ROI, can be calculated using formula for the area of intersection of two circles with radii R and $|z|\tan\beta$ and distance between the two centers r.

$$I(r,z) = I \quad \text{for } 0 < r < R - |z|\tan\beta,$$
$$I(r,z) = 0 \quad \text{for } r > R + |z|\tan\beta, \text{ and}$$
$$I(r,z) = \frac{I}{\pi(|z|\tan\beta)^2}\left(\phi(R,|z|\tan\beta,r) + \phi(|z|\tan\beta,R,r)\right) \text{ for } |r-R| < |z|\tan\beta.$$

where φ is function

$$\phi(\rho_1,\rho_2,d) = \rho_2^2\left(\arccos\frac{d^2+\rho_2^2-\rho_1^2}{2d\rho_2} - \frac{d^2+\rho_2^2-\rho_1^2}{2d\rho_2}\sqrt{1-\left(\frac{d^2+\rho_2^2-\rho_1^2}{2d\rho_2}\right)^2}\right),$$

representing the area of the circular segment cut off from the circle with radius ρ_2 by a chord of another circle with radius ρ_1 where d is the distance of circles centers. The expression for φ follows from the law of cosines.

Finally, $I(x,z) = I(|x|,z)$ for negative x.